Molecular Crystals and Liquid Crystals

ISSN: 1542-1406 (Print) 1563-5287 (Online) Journal homepage: http://www.tandfonline.com/loi/gmcl20

Thermal Treatment of Ultrathin Pentacene Thin-Film Transistors

Akira Heya & Naoto Matsuo

To cite this article: Akira Heya & Naoto Matsuo (2015) Thermal Treatment of Ultrathin Pentacene Thin-Film Transistors, Molecular Crystals and Liquid Crystals, 618:1, 83-88, DOI: 10.1080/15421406.2015.1075820

To link to this article: http://dx.doi.org/10.1080/15421406.2015.1075820

Published online: 07 Oct 2015.

Mol. Cryst. Liq. Cryst., Vol. 618: pp. 83–88, 2015

ISSN: 1542-1406 print/1563-5287 online
DOI: 10.1080/15421406.2015.1075820

Taylor & Francis
Taylor & Francis Group

Thermal Treatment of Ultrathin Pentacene Thin-Film Transistors

AKIRA HEYA* AND NAOTO MATSUO

Department of Materials Science and Chemistry, University of Hyogo, Himeji, Hyogo, Japan

Structural properties and influence of thermal treatment on electrical properties for organic thin-film transistor (OTFT) with 3 nm-thickness active layer pentacene were investigated. The pentacene film was preferentially oriented to (00l) of thin-film phase and carriers conducted thought standing molecules slantingly. The carrier mobility of the ultrathin OTFT was decreased, and the threshold voltage was shifted to negative direction by thermal treatment. For the ultrathin OTFT, the carrier conduction was affected by H_2O and O_2 because of change in the interface state and the hole localization state by adsorption of O_2 and H_2O and oxidation.

Keywords Ultrathin pentacene film; OTFT; Thermal treatment; Degradation; Oxidation

Introduction

Organic thin film transistors (OTFTs) have excellent features, low cost and flexibility compared with inorganic TFTs [1, 2]. So far, we had investigated the electrical characteristics of the pentacene OTFT with film thickness of 1, 3, 5, 10, and 50 nm [3]. When the thickness of pentacene film decreased to 3 nm, the on current (I_{on}) of the OTFT increased. It is considered that the triangle potential was formed at the interface between pentacene and SiO_2, and the quantum level was formed in the triangle potential for the ultrathin OTFT [3, 4]. It is expected that the carrier mobility of OTFT is improved by using quantum effect because the carrier scattering decreased at the interface between pentacene and SiO_2 [3, 4]. It is known that the electrical characteristics of OTFT are unstable because of the influence of H_2O and O_2 in air [5–10]. Therefore, it is important to clarify the degradation mechanism for the realization of stable OTFT.

In this paper, the structural properties and the influence of thermal treatment on the electrical properties of the ultrathin pentacene (3 nm thickness) OTFT were investigated for realization of stable organic devices.

*Address correspondence to Akira Heya, Department of Materials Science and Chemistry, University of Hyogo, 2167 Shosya, Himeji, Hyogo 671–2280, Japan. E-mail: heya@eng.u-hyogo.ac.jp

Color versions of one or more of the figures in the article can be found online at www.tandfonline.com/gmcl.

Experimental

Si(111) substrate (n-type, 0.2–0.4 Ωcm) was cleaned by using HF solution for 50 s. SiO_2 film (100 nm) was formed by a thermal oxidation in mixture of O_2 and H_2O moisture at 1000°C for 540 s. The pentacene film was deposited on the SiO_2/Si substrate by a thermal evaporation. The sample-holder temperature was room temperature (RT) and the base pressure was 2×10^{-4} Pa. The pentacene thickness was monitored using a quartz frequency unit. The thickness and deposition rate for pentacene film were 3 nm and 0.15 nm/s, respectively. An Au film was deposited by an electron beam evaporation as source and drain electrodes. The deposition rate and the thickness of Au film were 1 nm/s and 100 nm, respectively. The OTFT structure was fabricated using a metal-shadow [3]. The channel length (L) and width (W) of OTFT were 0.5 mm and 3 mm, respectively. Finally, the back side SiO_2 film was removed by a reactive ion etching.

The crystal structure of ultrathin pentacene/SiO_2/Si substrate was measured by GIXD (Grazing Incidence X-ray Diffraction). GIXD experiments were performed at the BL19B2 of SPring-8 with the approval of the Japan Synchrotron Radiation Research Institute (JASRI) (Proposal No. 2010A1853). The photon energy and beam spot size of X-ray were 10 keV and 0.15×0.50 mm^2, respectively.

The electrical properties were measured immediately after sample preparation at room temperature (RT) in air. Then the ultrathin OTFT was annealed at 95, 125, 150, 175, 200 and 225°C and 4 Pa for 1800 s. The electrical properties of the annealed OTFT were also measured at RT in air immediately after annealing.

In order to evaluate the oxygen content in the pentacene film after annealing, another sample with 5 nm thickness was annealed at 120, 200 and 320°C for 1800 s. The oxygen

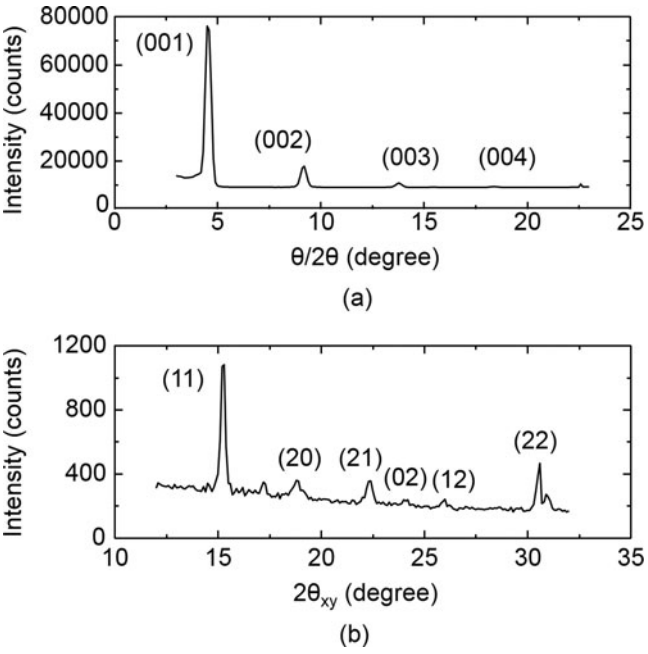

Figure 1. $\theta/2\theta$ mode XRD patterns (a) and in-plane GIXD patterns (b) of pentacene film with 3 nm thickness.

content was measured by Auger electron spectroscopy (AES). The acceleration voltage and beam spot in diameter were 10 kV and 1 μm, respectively.

Results and Discussion

$\theta/2\theta$ mode XRD and in-plane GIXD patterns of the pentacene film in ultrathin OTFT are shown in Figs. 1 (a) and (b), respectively. From the $\theta/2\theta$ mode XRD patterns, the ultrathin pentacene film was uniaxially oriented to (00l) of thin-film phase. For the in-plane GIXD pattern, various diffraction peaks were observed and the ultrathin pentacene was polycrystalline film. The first pentacene layer was strongly influenced by the surface of substrate [11] and deposition rate [12, 13]. This pentacene layer ruled the electrical conduction [14, 15]. From these results, the carriers transport thought standing molecules

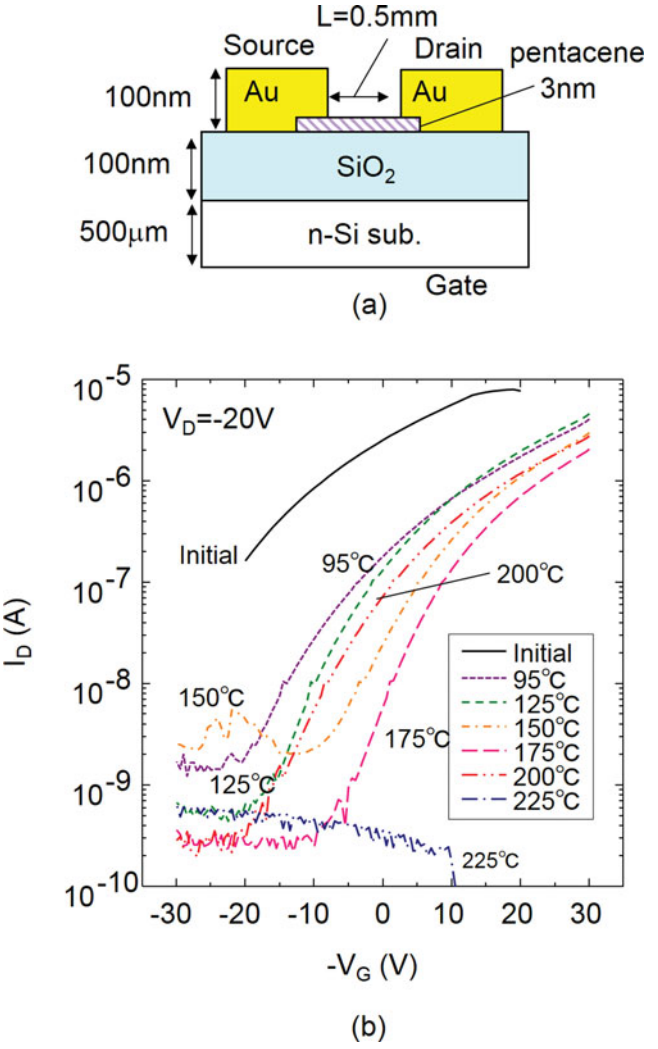

Figure 2. (a) Cross-sectional view of ultrathin OTFT. (b) I_D-V_G characteristics of the ultrathin OTFT. The electrical characteristics of OTFT were measured at RT in air.

slantingly via the grain boundary for the ultrathin OTFT. For the on current state, almost pentacene film became channel (accumulation) region [16].

The cross-sectional view of the ultrathin OTFT and the I_D-V_G characteristics are shown in Figs. 2 (a) and (b). The both on and off currents were decreased by annealing. It is considered that the carrier conduction was suppressed by H_2O and O_2 absorbed in grain boundary because H_2O and O_2 could be diffused to the accumulation region (two molecule-thick) [17] compared with a conventional OTFT. In addition, the ultrathin OTFT annealed at 225°C did not show transistor characteristics.

The dependences of mobility and threshold voltage (V_{th}) on annealing temperature are shown in Fig 3. After annealing at 95°C, the mobility and V_{th} changed from 0.07 to 0.04 cm^2/Vs and 19 to 1 V, respectively. When the annealing temperature increased, the mobility had a tendency to decrease. However, the mobility increased slightly at 125°C. It is known that physical adsorption of H_2O at the grain boundary of pentacene suppresses the carrier transport [7]. The thermal desorption of physical absorbed molecule increased with increasing annealing temperature. It is considered that the mobility was improved because H_2O molecules were desorbed by the annealing at 125°C. It seems that the mobility decreased because pentacene was oxidized by thermal treatment above 150°C. In general, the V_{th} relates to charge at interface between an active layer and gate insulator such as dangling bonds and OH radicals ($Si\text{-}OH + H_2O \rightleftharpoons Si\text{-}O^- + H_3O^+$) [3]. Therefore, it is shown that the ultrathin OTFT had many negative charges at interface because the fixed negative charges were easily generated by the above reaction of H_2O. After annealing, the V_{th} shifted to the negative direction because H_2O were easily desorbed by annealing for the ultrathin OTFT. However, the reason for increment of V_{th} at 200°C is under consideration.

From AES measurement, the oxygen contents in the initial and pentacene films annealed at 120, 200 and 320°C were 8, 14, 15 and 22 at.%. The oxygen content increased with increasing of annealing temperature. Although desorption of H_2O molecule increased,

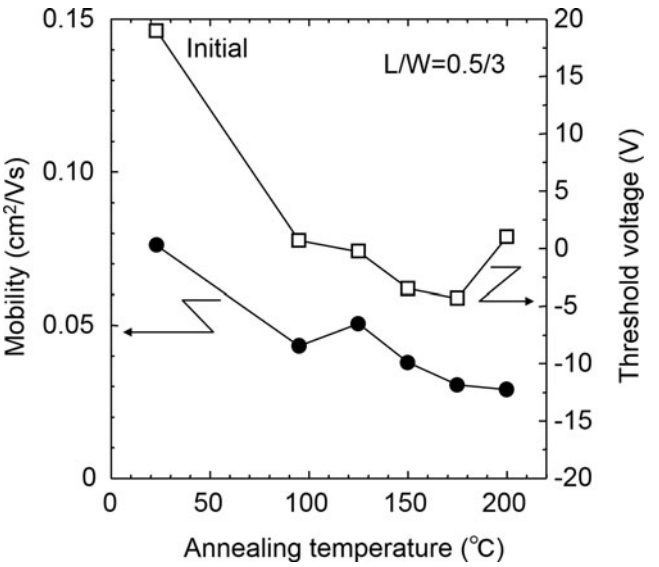

Figure 3. Mobility and V_{th} as a function of annealing temperature. The mobility was estimated from linear region of I_D-V_D characteristics by assuming that carrier transport was band conductivity. The V_{th} was estimated from tangent of $\sqrt{I_D}$-V_D characteristics.

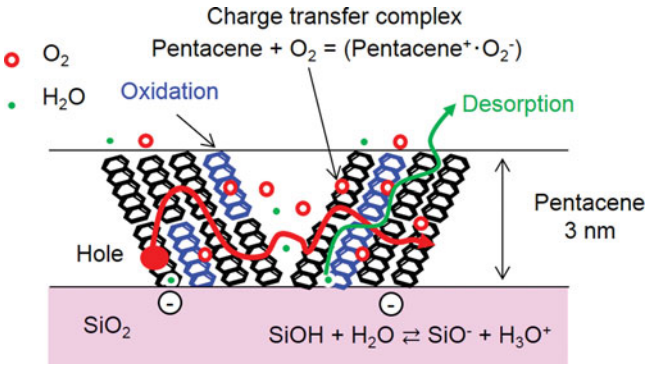

Figure 4. Schematic diagram of influence of H_2O and O_2 on carrier conduction in the ultrathin OTFT after annealing. The carrier conduction was suppressed by H_2O and O_2 on film surface and at the interface. A part of pentacene molecules was oxidized in high-temperature annealing.

the mobility was decreased by oxidation for the high-temperature treatment. It is shown that change in the mobility and V_{th} relates to oxygen in the pentacene film and the interface between pentacene film and SiO_2.

Finally, the influence of H_2O and O_2 on the carrier conduction in ultrathin OTFT (Figure 4) is discussed. When the O_2 adsorbs on surface of ultrathin pentacene, the electrons in pentacene transfer to the highest occupied molecular orbital level of O_2 molecules (12eV) [18]. The band discontinuities induce in channel region. In addition, the carrier scattering is increased by band discontinuities due to pentacene oxidation. In addition, H_2O and O_2 adsorbed in channel affect the hole localization state. The ultrathin OTFT is expected as O_2 sensor because those effects are sensitivity to oxygen.

Conclusion

The ultrathin pentacene film (3 nm thickness) was preferentially oriented to (00l) of thin-film phase and the carrier conducted thought standing molecules in channel region. The mobility and V_{th} of the ultrathin pentacene OTFT were changed by annealing due to oxidation or O_2 and H_2O desorption. For the ultrathin OTFT, the effects of H_2O and O_2 on carrier conduction were strong because the interface state and hole localization state were changed by O_2 and H_2O adsorption and oxidation.

The authors are grateful to T. Koganezawa in Japan Synchrotron Radiation Research Institute (JASRI) for GIXD measurement.

References

[1] Kymissis, I., Dimitrakopoulos, C. D., & Purushothaman, S. (2001). *IEEE Trans. Electron Devices*, *48*, 1060.
[2] Forrest, S. R. (1997). *Chem. Rev.*, *97*, 1793.
[3] Heya, A. & Matsuo, N. (2010). *Extended Abstracts of the 2010 International Conference on Solid State Devices and Materials (SSDM)*, P-10–18.
[4] Matsuo, N. & Heya, A. (2011). *IEICE Electronics Express*, *8*, 360.
[5] Hu, Y., Dong, G., Hu, Y., Wang, L., & Qiu, Y. (2006). *J. Phys. D, Appl. Phys.*, *39*, 4553.
[6] Goldmann, C., Gundlach, D. J., & Batlogg, B. (2006). *Appl. Phys. Lett.*, *88*, 063501.

[7] Yokoyama, T., Park, C. B., Nishimura, T., Kita, K., & Toriumi, A. (2008). *Jpn. J. Appl. Phys.*, *47*, 3643.
[8] Sekitani, T., Hizu, K., & Someya, T. (2006). *IEICE Technical Report OME2006-120*, p. 65.
[9] Zhu, Z-T., Mason, J. T., Dieckmann, R., & Malliiaras, G. G. (2002). *Appl. Phys. Lett.*, *81*, 4643.
[10] Kumaki, D., Umeda, T., & Tokito, S. (2008). *Appl. Phys. Lett.*, *92*, 093309.
[11] Killampalli, A. S., & Engstroma, J. R. (2006). *Appl. Phys. Lett.*, *88*, 143125.
[12] Pratontep, S., Brinkmann, M., Nu¨esch, F., & Zuppiroli, L. (2004). *Phys. Rev., B 69*, 165201.
[13] Stadlober, B., Haas, U., Maresch, H., & Haase, A. (2006). *Phys. Rev., B 74*, 165302.
[14] Dinelli, F., Murgia, M., Levy, P., Cavallini, M., Biscarini, F., & de Leeuw, D. M. (2004). *Phys. Rev. Lett.*, *92*, 116802.
[15] Shehu, A., Quiroga, S. D., D'Angelo, P., Albonetti, C., Borgatti, F., Murgia, M., Scorzoni, A., Stoliar, P., & Biscarini1, F. (2010). *Phys. Rev. Lett.*, *104*, 246602.
[16] Kiguchi, M., Nakayama, M., Fujiwara, K., Ueno, K., Shimada, T., & Saiki, K. (2003). *Jpn. J. Appl. Phys.*, *42*, L1408.
[17] Kim, W. J., Kim, C. S., Jo, S. J., Lee, S. W., & Lee S. J. (2007). *Electrochem. Solid-State Lett.*, *10*, H1.
[18] Heya, A., Matsuo, N., & Konaganezawa, T. (2011). *Abst. 2011 International Meeting for Future of Electron Devices, Kansai (IMFEDK)*, pp.123–124.